International Journal of Applied Science; Vol. 5, No. 1; 2022
ISSN 2576-7240 E-ISSN 2576-7259
https://doi.org/10.30560/ijas.v5n1p8

LQR Based On Optimized Tuning PD Controller For AVR System

Eman H. Jadoua[1], Noor M. Diwood[1] & Yasameen F. Azeez[1]

[1] Al-Farabi University College, Iraq

Correspondence: Eman H. Jadoua, Al-Farabi University College, Department of Computer Engineering, Baghdad, Iraq. E-mail: emanhassony06@gmail.com, noormudam@alfarabiuc.edu.iq, dr.yasmeen.fawzi@alfarabiuc.edu.iq

Received: July 10, 2022; Accepted: September 1, 2022; Published: September 12, 2022

Abstract

This study presents a Linear Quadratic Regulator (LQR) based on an optimizing PD controller to improve the dynamic performance of an automatic voltage regulation (AVR) system. Biogeography-based optimization (BBO) is used to adjust the controller gains, and the Mean Absolute Percentage Error (MAPE) cost function is used to ensure effective performance. To demonstrate the advantages of the suggested controller, a transient study was conducted and compared to a standard PD, LQR, and then used PD-LQR in terms of (Rising time, Settling time, Max Overshoot, and Peak time). Finally, simulations demonstrated that the PD-LQR gives satisfactory outcomes and a quicker reaction, which was evidently represented in the recommended controller's strong and steady performance in enhancing the transient analysis of the AVR system.

Keywords: AVR system, Optimization Techniques, PD Controller, LQR, PD-LQR Controller

1. Introduction

The system has a nominal value level for supplying power network voltages. Any change in the given voltage value will affect all distributed power networks' dynamics. This condition of altering values will have an impact on the system's performance and longevity. The impact will be felt on the electrical grid and, eventually, on the actual system that delivers the necessary voltages. To overcome this problem, an automatic voltage regulator (AVR) is used[1]. An AVR, as the name indicates, is a device used in power plants to maintain target voltage levels despite fluctuations. It works by first the excitation section's voltage value being stabilized, then managing the excitation voltage value to regulate the output producing voltage in order to provide dependable and a stable voltage providing system[2]. Oscillation, overshoot, and a value error in the steady-state are some of the issues that the AVR has in its output response. Many control systems based on optimal control, robust control, and adaptive control have been investigated in the literature for implementing and increasing the dynamic responsiveness of an AVR system.

Conventional PID is without a doubt the most common because to its stable performance independent of system parameter changes and structural simplicity, just three control parameters—proportional gain, integral gain, and derivative gain—need to be adjusted[3]. To create a robust response, a genetic algorithm (GA) is paired with and PSO, whereas in [4], a The connection between fuzzy and PID controller combines fuzzy with differential (FD), fuzzy with integration (FI), and fuzzy with proportional (FP) (HGAPSO). The FOPID controller, which has been proposed in [2], offers a significant degree of freedom when tweaking its parameters using WOA. When compared to a traditional PID controller, the FOPID controller exhibits different time response properties. By resolving algebraic recombinant equations, one may create state feedback control in the simplest way possible using a linear quadratic (LOR) structured technique. Selecting settings for this method is still a trial-and-error process. Make specific changes to the weight matrices' Q and R elements[5].

In this paper, the BBO for adjusting LQR controller gains and PD parameters. When this method is used, it produces fast and accurate results for (PD-LQR) controller gains, as well as ability to tune its gains with a lot of freedom. Finally, the time response properties of the PD-LQR controller are compared to those of the traditional PD and LQR controllers. The following is how the paper is structured: Section 2 describes the AVR system, Section 3 describes the LQR controller, and Section 4 shows the proposed BBO method. Results from the simulation and discussion are presented in Section 5; the study's conclusion is covered in Section 6.

2. AVR System Model

The four parts of the AVR system are the amplifier, exciter, generator, and sensor. As illustrated in Figure 1, each of these parts has a first-order transfer function. Each transfer function's known time and gain constants in the AVR system are the parameters (T and k). Table 1 lists the values of the constants utilized in this investigation.

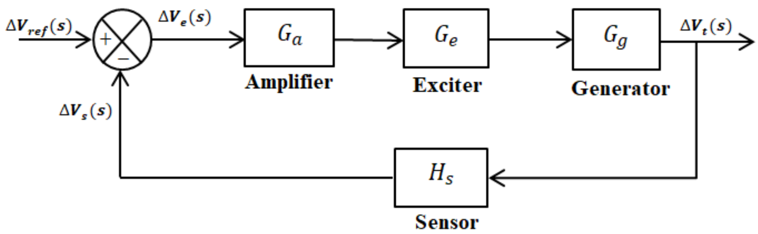

Figure 1. AVR system block diagram

2.1 The Amplifier Model

A gain and a time constant are used to simulate the transfer function of an amplifier.

$$G_a = \frac{K_a}{1+sT_a} \tag{1}$$

where the amplifier's time constant (T_a) and gain (K_a) are respectively. T_a is between 0.02 and 0.1 sec, while K_a values are between 10 and 40.

2.2 The Exciter Model

A gain and time constant are used to simulate the transfer function of an exciter:

$$G_e = \frac{K_e}{1+sT_e} \tag{2}$$

where K_e and T_e are the exciter's gain and time constant. K_e values vary from one to two, while T_e values range from 0.4 to 1.0 sec.

2.3 The Generator Model

A generator's transfer function is described by a gain and a time constant provided by:

$$G_g = \frac{K_g}{1+sT_g} \tag{3}$$

where, K_g and T_g represent the gain and time constant of the generator and load are dependent. The values of K_g are in the range of (0.7 to 1.0) and T_g in the range of (1 to 2) seconds from maximum load to zero loads.

2.4 The Sensor Model

A gain and a time constant are used to represent the transfer function of a sensor and are as follows:

$$G_s = \frac{K_s}{1+sT_s} \tag{4}$$

where K_s and T_s stand for the sensor's gain and time constant, respectively. K_s ranges from (0.02 to 1.0) and T_s from (0.01 to 2.2) seconds.

Table 1. AVR component performance values

AVR Component	Parameters	values
Amplifier	K_a	10
	T_a	0.1
Exciter	K_e	1
	T_e	0.4
Generator	K_a	1
	T_a	1
Sensor	K_s	1
	T_s	0.01

The following will be the closed loop transfer function[6]:

$$\frac{\Delta V_t(s)}{\Delta V_{ref}(s)} = \frac{0.1s+10}{0.0004\,s^4+0.0454\,s^3+0.555\,s^2+1.51\,\text{s}+11} \tag{5}$$

Eq.(5) can be reduced to second order (T.F.) by utilizing the error reduction strategy. This is accomplished by converting the higher order transfer function to the lower order transfer function in the following manner:

$$\frac{0.1s+10}{0.0004\,s^4+0.0454\,s^3+0.555\,s^2+1.51\,\text{s}+11} = \frac{p_1 s+p_0}{s^2+r_1 s+r_0} \tag{6}$$

By cross multiplying Eq.(7) and comparing terms with similar powers of (s) on both sides:

$$(0.1s+10)(s^2+r_1 s+r_0) = (0.0004\,s^4+0.0454\,s^3+0.555\,s^2+1.51\,\text{s}+11)(p_1 s+p_0) \tag{7}$$

By solving the simultaneous linear equations that obtained from Eq.(8) the value of unknown parameters are:

$p_1 = -1.69,\ p_0 = 22.86,\ r_1 = 1.341,\ r_0 = 25.14$

The obtained transfer function become:

$$G_r = \frac{-1.69s+22.86}{s^2+1.341s+25.14} \tag{8}$$

3. Control Methods

The Proportional Derivative (PD) and Linear Quadratic Controller (LQR) control techniques are used to regulate the AVR system. In this section, PD and LQR controllers are discussed and then will combine PD-LQR to enhance the performance of the AVR system. To employ a controller, the system must be observable and controllable for all states in the state-space model.

3.1 PD Controller

A feedback controller is a Proportional Derivative controller. Various ways are being used to adjust K_p , and K_d the proportional, and derivative gains of a PD controller, tuning using the trial and error or Ziegler-Nichols as a traditional method. In this paper PD controller, tuning using the BBO algorithm. PD Controller's transfer function is as follows:

$$u(t) = K_p e(t) + K_d \frac{de}{dt} \tag{9}$$

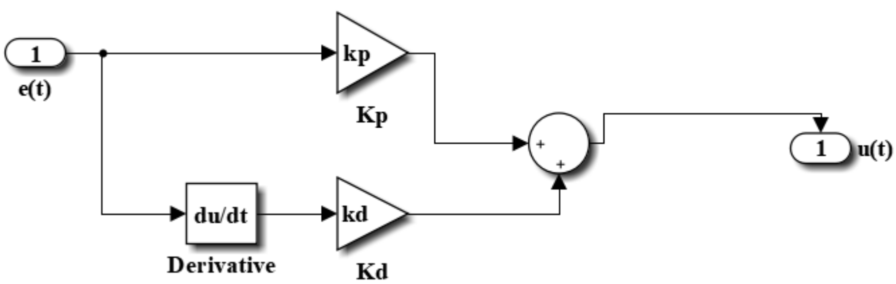

Figure 2. PID controller Simulink blocks

The system is controlled by comparing the produced error to the reference input and measured output. K_p and K_d are set for the controller's optimal performance.

3.2 Linear Quadratic Regulator Controller

The following is a description of the state space representation of a linear time-invariant (LTI) system.

$$\dot{\boldsymbol{x}}(t) = \boldsymbol{A}\boldsymbol{x}(t) + \boldsymbol{B}u(t) \tag{10}$$

$$\text{y(t)} = \text{Cx(t)} + \text{Du(t)} \tag{11}$$

Where the state vector x(t), the output vector y(t), and the control vector u(t) are all vectors. Equation (12) is a form that may be used to define the linear state feedback rule in the LQR technique.

$$u(t) = -\boldsymbol{K}\boldsymbol{x}(t) \tag{12}$$

K is the matrix of the state feedback. In order to minimize the quadratic performance index, which is specified in equation (13), the LQR control issue may be described as the search for the best linear state feedback law:

$$J = \int_0^\infty [x(t)^T \boldsymbol{Q} x(t) u(t)^T \boldsymbol{R} u(t)] dt \tag{13}$$

Where Q and R are the state matrix and input matrix's respective positive definite and semidefinite weight matrices. When you resolve: then get the control gain matrix K.

$$K = R^{-1} B^T P \tag{14}$$

where P is the algebraic Riccati equation's solution as a result of:

$$A^T P + PA - PBR^{-1} B^T + Q = 0 \tag{15}$$

Figure (3) depicts the block diagram of this ideal LQR controller, which comprises of the LQR controller and several optimization algorithms used to get the ideal weighting matrices for the LQR controller.

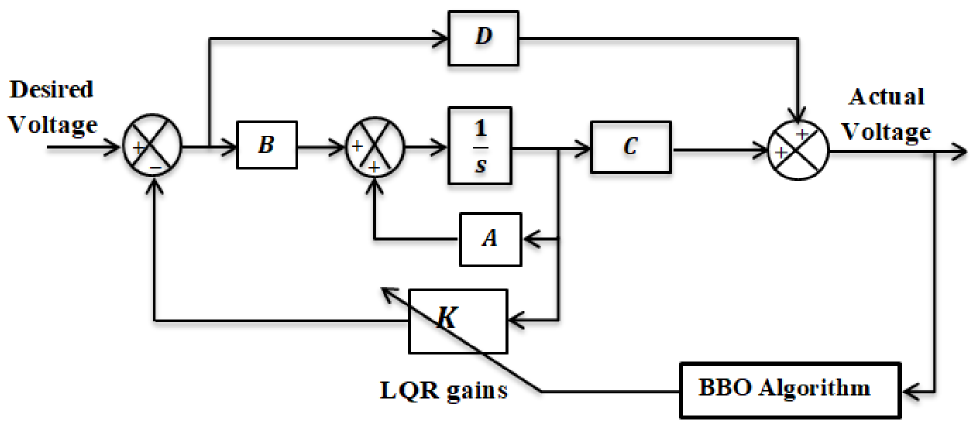

Figure 3. The Block Diagram Of Tuning LQR Based BBO Controller

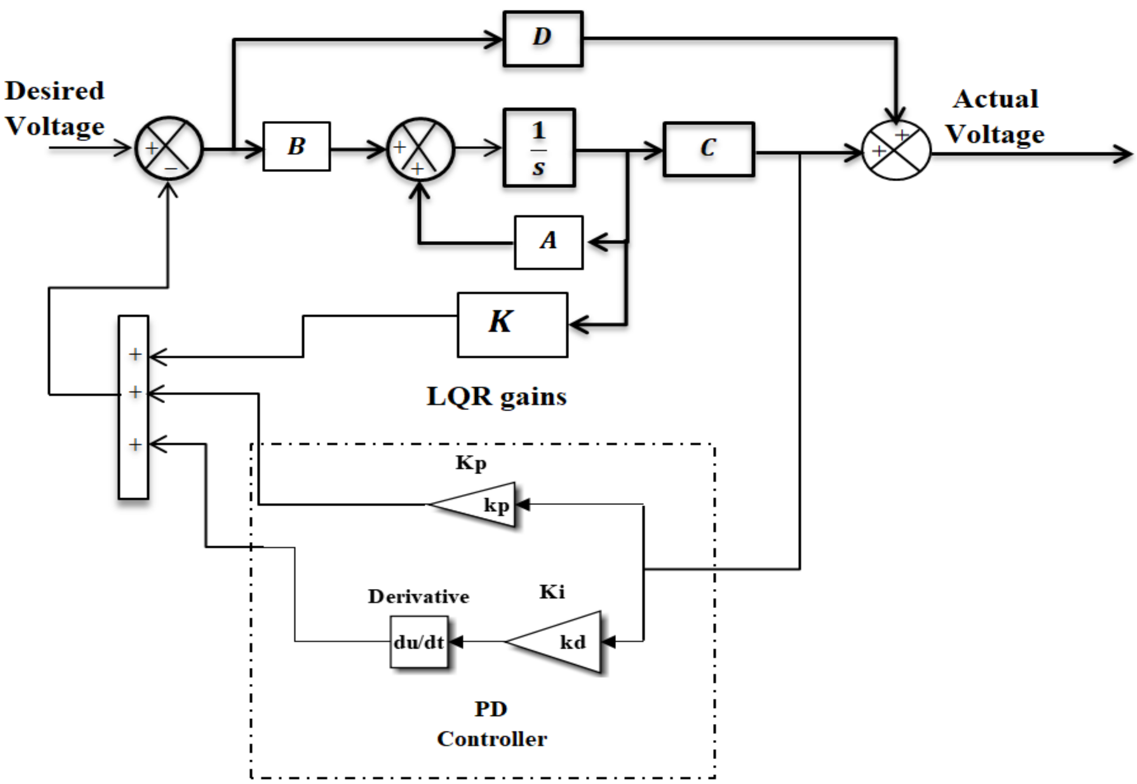

Figure 4. The Block Diagram Of (PD-LQR) Controller.

3.3 PD-LQR Controller

To greatly improve the response performance of existing available controllers, a combination of the LQR controller with the PD controller is recommended. A proportional component for a PD controller can boost reaction speed, lowering the amount of time necessary to obtain the desired output. To balance the desired output, another gain parameter is required. This controller's downside is that it has a tendency to enhance overshoot, making the system more unstable than before. As a result, the derivative controller element in the proposed (PD-LQR) controller decreases overshoot and smoothes and stabilizes the response. An integrated controller is not included in this combination since its addition to a LQR controller will alter the system output. Figure 4 depicts the (PD-LQR) controller flow.

4. BBO Algorithm

The BBO algorithm was initially developed in 2008 by D. Simon [10]. It is based on the concept of biogeography and mathematically depicts species migration from one island to another and how this shift happens from fewer areas to more appropriate places to live. In terms of biogeography, species move from one island to another depending on the habitat suitability index (HSI), which in turn depends on a variety of factors including food variety, temperature, land area, and water supplies. These qualities are referred to as Suitability-Index-Variables (SIV). SIV identifies the adjusted parameter's quantity, whereas HSI is comparable to the cost or fitness function in other population-based optimization techniques [11]. BBO typically involves two steps: information exchange (migrations) and mutation.

1) Migration

The migration of species across habitats takes place when HSI of habitats is low or if more species concentrate in the same habitat since the environment with the greatest HIS is the best for living species. Emigration refers to the preceding procedure. However, migration is the term used when a species moves to an environment with a high HSI. Both used the term "migration" [11, 12]. The method of migration used to modify the solution (Hi) by incorporating elements from a different solution (Hj), which may be identified by:

$$H_i(SIV_k) \leftarrow H_j(SIV_k) \tag{16}$$

A H_i answer The emigration rate μi and the immigration rate λi can be used to calculate immigration or emigration [11]. μi and λi are determined using Equations (24) and (25), respectively, for each habitat that has a unique value.

$$\mu_i = \frac{k_i}{n} E \tag{17}$$

$$\lambda_i = \left(1 - \frac{k_i}{n}\right) I \tag{18}$$

Where n stands for population size, I and E stand for maximum immigration and emigration rates, respectively, and k_i is the rank Hi following evaluation.

2) Mutations

The probabilistic element (mutation) utilized to improve population variety and provide new characteristics of a solution chosen at random by changing one or more of its SIV [10]. The mutations of the ith habitat were depicted in equation (19).

$$M_i = m_{max}\left(1 - \frac{P_i}{P_{max}}\right) \tag{19}$$

Where Pi is the habitat Hi existence probability and mmax which is determined by the user and represents the coefficient of mutation.

5. Simulation Results

The simulation results for the proposed controller are shown in this part; all simulations are performed using (MATLAB/Simulink) to assess the performance of the (PD-LQR) controller based on BBO and compare it to the traditional PD and LQR controllers adjusted using BBO. In addition, the initial BBO parameters are mentioned in Table 2.

Table 2. The BBO algorithm's parameters

parameters of BBO	Number of generations	Probability of Mutation	n (Habitats)	SIV	E	I	Min Domain	Max Domain
value	10	0.06	20	5	1	1	0	10

A performance index is then utilized to assess the controller's performance in tracking the intended output value on a continuous basis. Figure 5 displays the system's block diagram. In this study, Mean Absolute Percentage Error (MAPE) was chosen as a fitness function and employed in BBO to adjust the controller gains and provide a stable system response. It is illustrated in (20) [13].

$$MAPE = \frac{1}{n}\sum_{t=0}^{n}\frac{(V_t - V_{ref})}{V_t} \tag{20}$$

Figure 4 displays the AVR system's open loop responses.

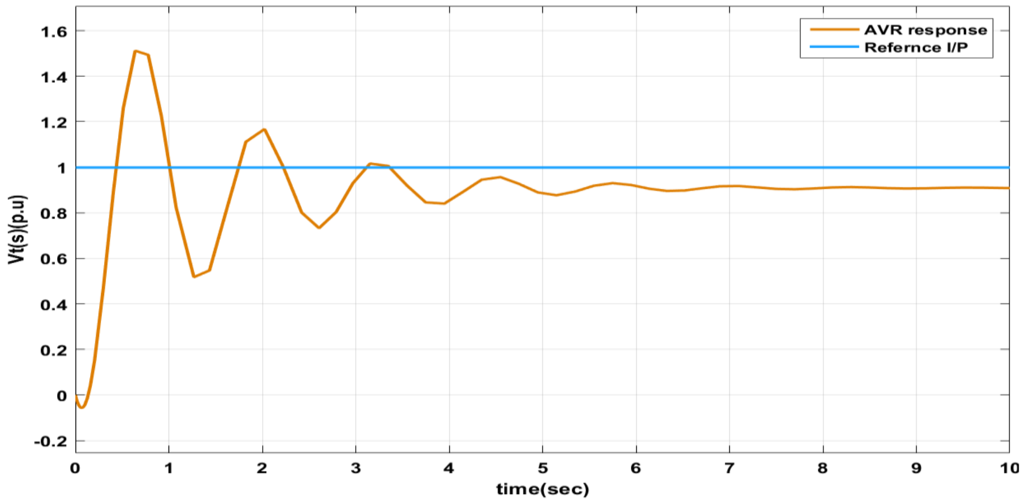

Figure 5. The AVR system's original terminal voltage step response change

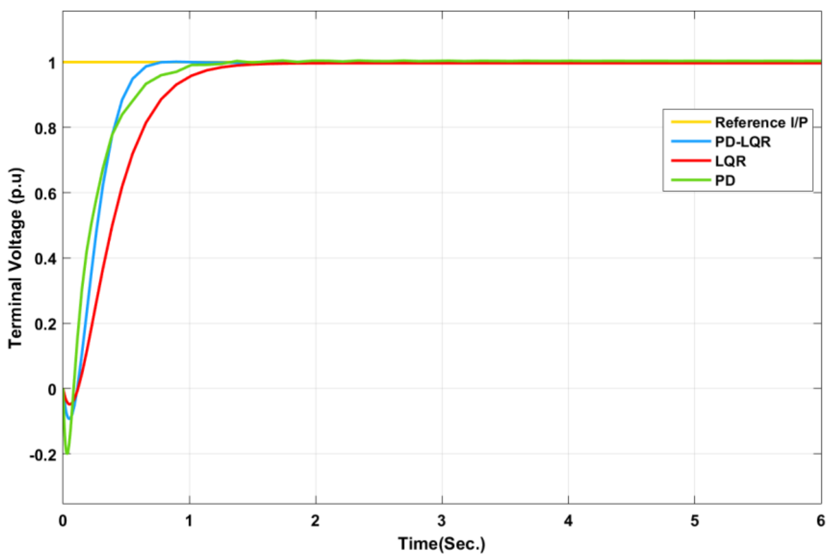

Figure 6. Responses to terminal voltage for suggested controllers

Figure 4 shows the response change of the abovementioned AVR system. It can be seen that the system exhibits a striking inaccuracy at steady-state and begins with severe oscillations. When considering the operating voltage on the order of kilovolts, such a response is utterly inappropriate in power systems and cannot be permitted to occur. To improve the transient response of the AVR system and eliminate the steady-state error, controllers such as PD, LQR, and then used (PD-LQR) will be installed in the concerned system. Figure 6 presents the controllers' response to the system (PD, LQR, and PD-LQR), and Table 3 lists the gains of the best controllers in order to compare the system performance of the LQR controller with classical PD and PD-LQR (adjusted using BBO). Table 4 displays the step response results controllers.

The values for the (LQR & PD) Gains tuned using BBO are as follows:

PD controller (P=0.89, and D=0.087)

LQR controller ($K_1 = 8.94,$ and $K_2 = 1.92$)

PD-LQR controller (P=0.89, D=0.087, $K_1 = 8.94,$ and $K_2 = 1.92$)

Table 3. Results of step responses for suggested controllers based on BBO

Controllers using BBO	Rise Time(s)	Settling Time(s)	Peak Time(s)	M_p%
PD	**0.48**	**0.93**	**2.34**	**0.47**
LQR	**0.63**	**1.19**	**4.02**	**0**
PD-LQR	**0.34**	**0.63**	**0.89**	**0.098**

The suggested controller varies from traditional PD and LQR controllers in the step response analysis. This is because of the combined effects of the controllers' effects on system response, which have been demonstrated to have a fast settling time that is 67% faster than the traditional PD controller and 53% faster than the LQR, as well as a small overshoot that results in a stable and effective desired response.

6. Conclusions

Based on the AVR mathematical model, the PD and LQR control techniques may both be used to control the AVR system. Different controller settings were tuned using the BBO algorithm with the goals of minimizing error and following the expected response. According to the controller simulation findings, the combined (PD-LQR) controller is necessary for greater performance since it responds faster and reduces overshoots, which are problems that the AVR points experience and show in its output response.

Reference

[1] Ray, N. K., Mohapatra, S. K., & Dash, S. S. (2020, July). Gravitational Search Algorithm for Optimal Tunning of controller parameters in AVR system. In *2020 International Conference on Computational Intelligence for Smart Power System and Sustainable Energy (CISPSSE)* (pp. 1-6).

[2] Abood, L. H., & Bashra, K. O. (2021). Design of fractional order PID controller for AVR system using whale optimization algorithm. *Indonesian Journal of Electrical Engineering and Computer Science* 23.3, (2021), 1410-1418.

[3] Chatterjee, S., & Mukherjee, V. (2016). PID controller for automatic voltage regulator using teaching–learning based optimization technique. *International Journal of Electrical Power & Energy Systems* 77 (2016), 418-429.

[4] H. Shayeghi, A. Y., & Hashemi, Y. (2015). Optimal design of a robust discrete parallel FP+ FI+ FD controller for the automatic voltage regulator system. International Journal of Electrical Power & Energy Systems, (67), 66-75. https://doi.org/10.1016/j.ijepes.2014.11.013

[5] Karam, E. H., & Noor, M. M. (2017). Improve Linear Quadratic Regulator by Particle Swarm Optimization Algorithms for Two Wheeled Self Balancing Mobile robot." *Iraqi Journal for Electrical And Electronic Engineering, 13*(2).

[6] B. Ozgenc, M. S. A., & Altas, I. H. (2020). A Hybrid Optimization Approach to Design Optimally Tuned PID Controller for an AVR System. International Congress on Human-Computer Interaction, Optimization and Robotic Applications (HORA), 2020, pp. 1-5. https://doi.org/10.1109/HORA49412.2020.9152898.

[7] Karam, E. H., Noor, S. Abdul-Jaleel, & Basma, J. S. (2020). Design of hybrid Neuro-Robust deadbeat controller for higher order linear systems based on optimized mixed reduction method. *International Review of Applied Sciences and Engineering, 11*(3), 251-260.

[8] Maghfiroh, H., Ataka, A., Wahyunggoro, O., & Cahyadi, A. I. (2013, November). Optimal energy control of

dc motor speed control: Comparative study. In *2013 International Conference on Computer, Control, Informatics and Its Applications (IC3INA)* (pp. 89-93).

[9] Brian, R. C. (2008). The Design of PID Controllers using Ziegler Nichols Tuning" March 2008.

[10] Simon, D. (2008). Biogeography-based optimization. *IEEE Transactions on Evolutionary Computation*, *12*(6), 702-713.

[11] Mohammed, S., & Mohamed, F. K. (2012). Application of Biogeography based optimization in tuning a PID controller for nonlinear systems. IEEE, 2012.

[12] Haiping, Ma, Dan, Simon, Patrick, S., Yang, Z. L., & Fei, M. R. (2017). Biogeography-Based Optimization: A 10-Year Review. *IEEE Transactions on Emerging Topics in Computational Intelligence, 1*(5), OCTOBER 2017.

[13] Jadoo, E. H., & Ekhlas, H. K. (2020). FPGA IMPLEMENTATION OF SECOND ORDER SLIDING MODE BASED ON ST ALGORITHM FOR TYPE I DIABETES. *Journal of Engineering and Sustainable Development (JEASD)* 24. Special_ Issue_2020.